Electronic Supplementary Material (ESI) for Nanoscale Advances.


## Supplementary Materials

# Tilt grain boundaries in $WS_2$ from the low to high misorientation angles

Da Ke, Jinquan Hong, and Yubo Zhang*

*Minjiang Collaborative Center for Theoretical Physics, College of Physics and Electronic Information Engineering, Minjiang University, Fuzhou 350108, China*

Corresponding email address: yubo.drzhang@mju.edu.cn

## Contents

## 1. Other details of the coincidence site lattice (CSL) theory for $WS_2$

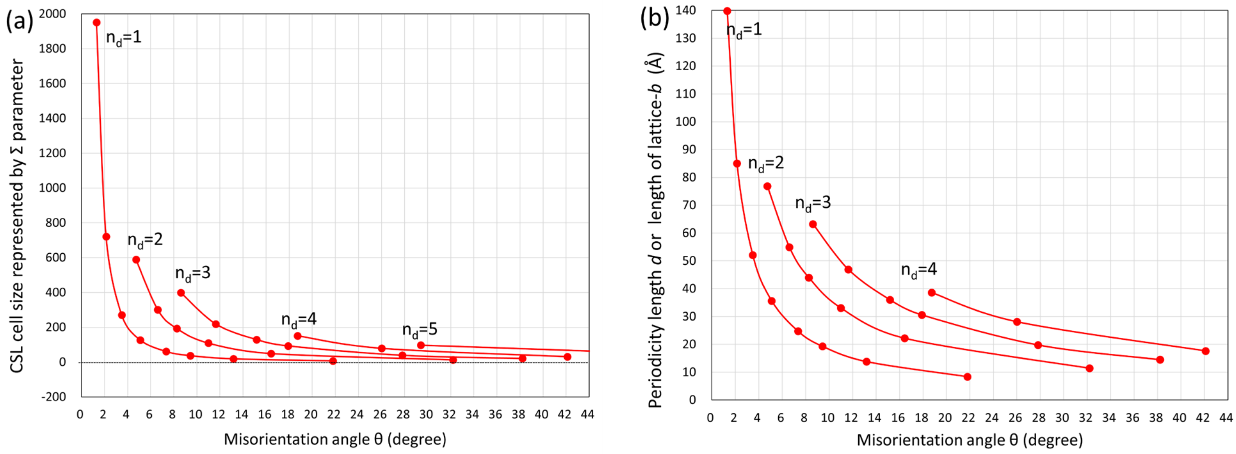


**Figure S1. (a)** The CSL cell size as a function of the misorientation angles. **(b)** Periodicity length as a function of misorientation angles. The systems are grouped based on the GB families $n_d$.

## 2. First-principle simulation details

The first-principle simulations are mainly performed using the SIESTA code [1]. The electron-ion interaction is represented by pseudopotentials in the norm-conserving method. The valence electrons of W $5d^4 6s^2$ and S $3s^2 3p^4$ are explicitly considered. For the basis set, the single-zeta (SZ) basis is used for the structural relaxation, and the "standard" choice of double-zeta plus polarization (DZP) is later adopted for calculating the electronic properties. Exchange-correlation functional is in the form of Perdew-Burke-Ernzerhof [2] generalized gradient approximation. Structural optimization is the key to getting the low-energy motifs of the GB models. It is a difficult task and is performed carefully. The convergence criteria are 0.1 eV/Å for the force on atoms.

For cross-checking, calculations are also performed for a few selected systems using the all-electron FHI-aims code [3]. Formation energies from Siesta and FHI-aims code, shown in Figure S2, agree well with each other.

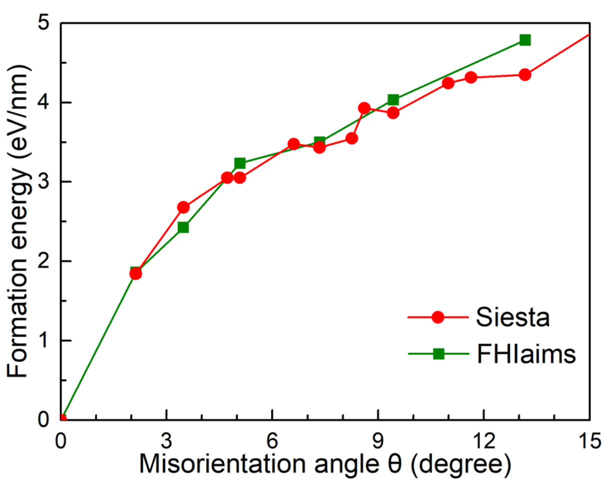


**Figure S2.** Formation energies of a few selected GB models. The results by the Siesta and FHI-aims are compared.

## 3. Relaxed structural models

### 3.1. The family of $n_d = 1$

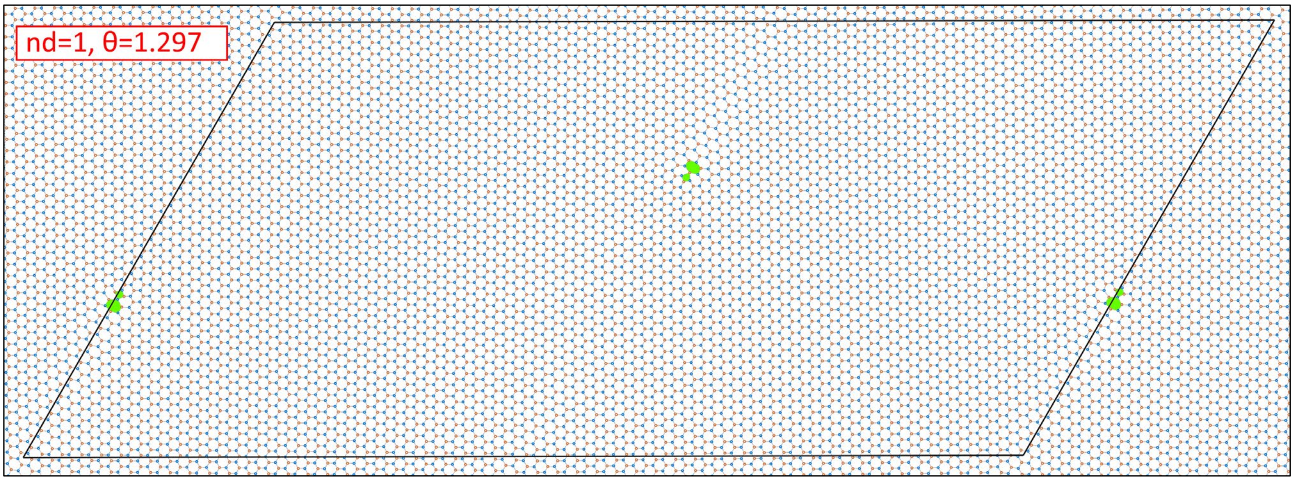


**Figure S3-1-1.** GB model of family $n_d = 1$ and misorientation angle $\theta = 1.297^{\circ}$. The relaxed simulation cell sizes are $a = 277.35$ Å and $b = 139.81$ Å.

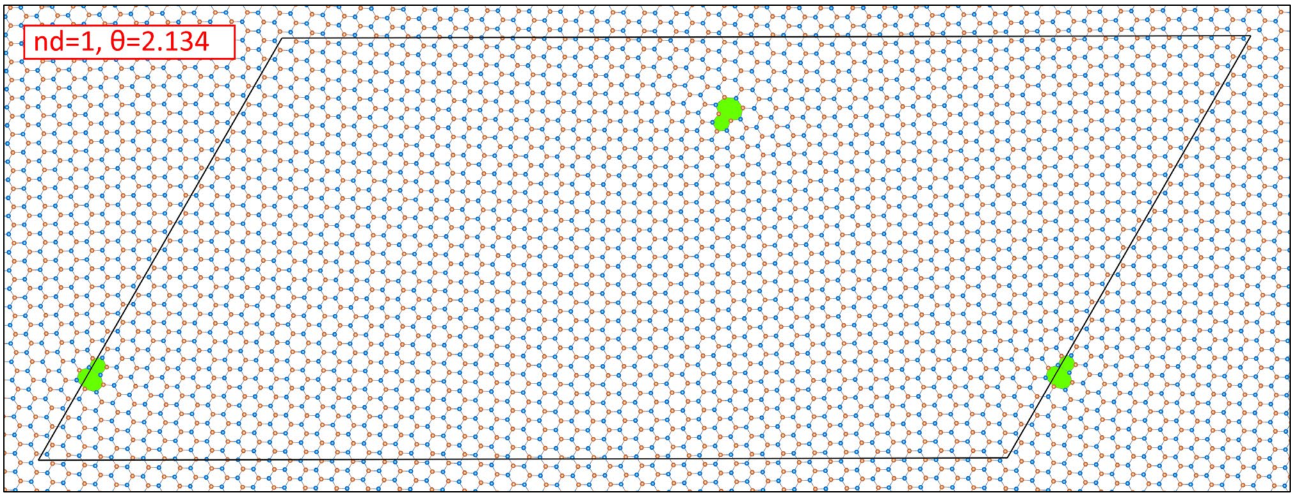


**Figure S3-1-2.** GB model of family $n_d = 1$ and misorientation angle $\theta = 2.134^{\circ}$. The relaxed simulation cell sizes are $a = 169.08$ Å and $b = 85.01$ Å.

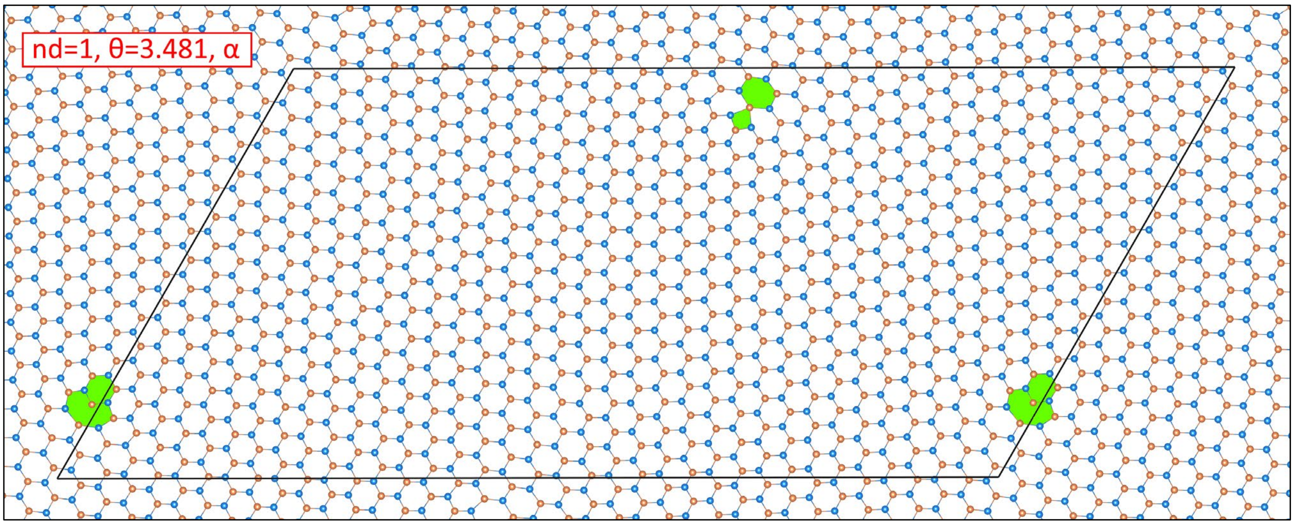


**Figure S3-1-3a.** GB model of family $n_d = 1$ and misorientation angle $\theta = 3.481^{\circ}$. The distorted dislocations are 4|6 and 6|8 rings. The relaxed simulation cell sizes are $a = 103.75$ Å and $b = 52.10$ Å.

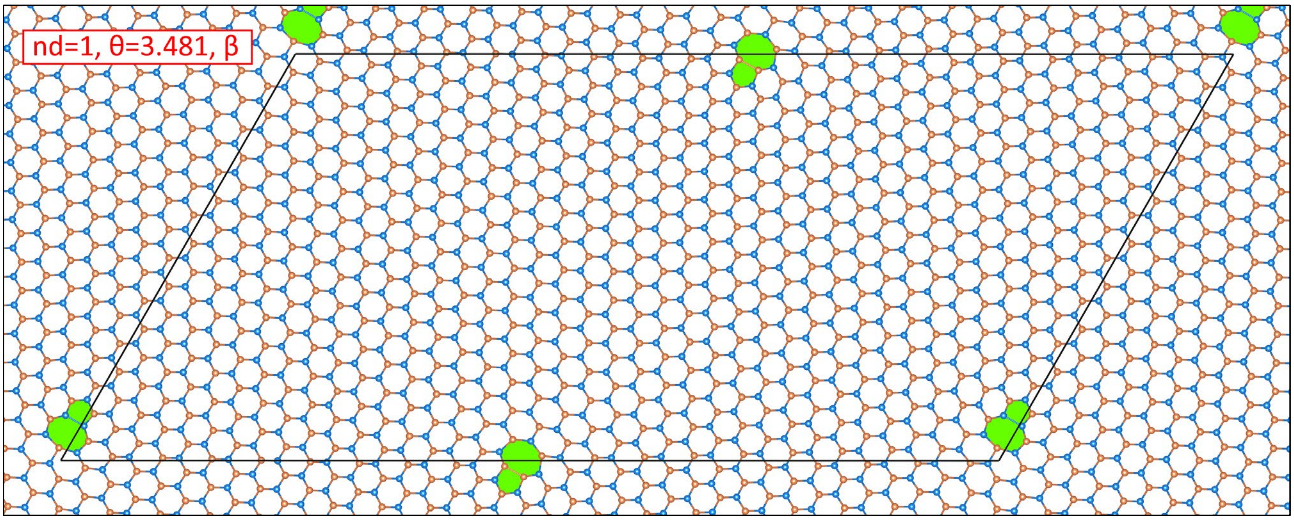


**Figure S3-1-3b.** GB model of family $n_d = 1$ and misorientation angle $\theta = 3.481^{\circ}$. The distorted dislocations are 5|7 rings. The relaxed simulation cell sizes are $a = 104.15$ Å and $b = 52.10$ Å.

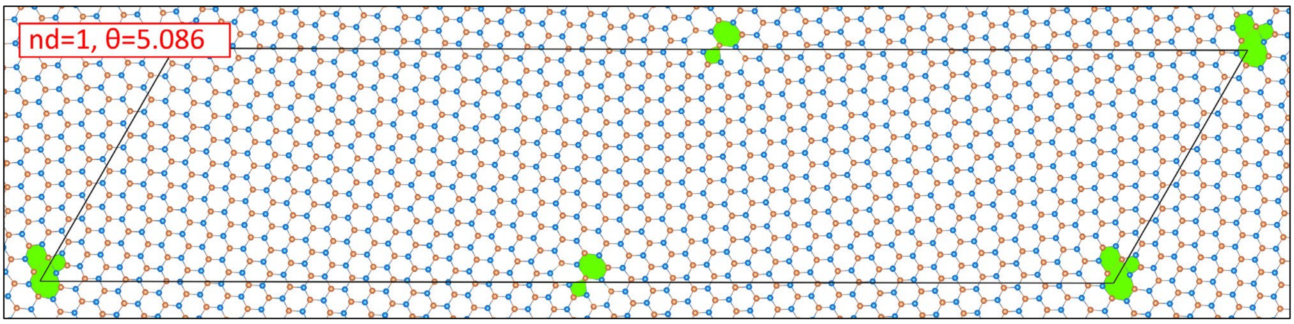


**Figure S3-1-4.** GB model of family $n_d = 1$ and misorientation angle $\theta = 5.086^{\circ}$. The relaxed simulation cell sizes are $a = 142.75$ Å and $b = 35.65$ Å.

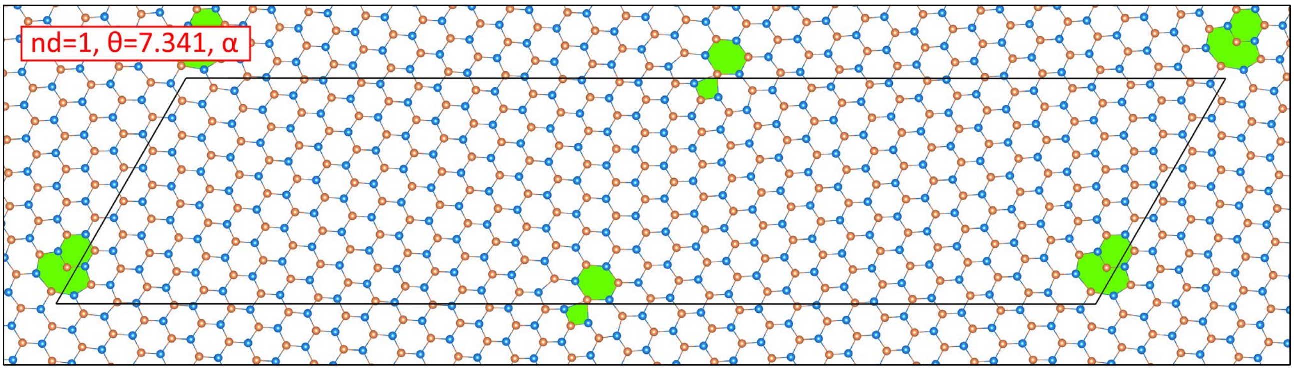


**Figure S3-1-5a.** GB model of family $n_d = 1$ and misorientation angle $\theta = 7.341^{\circ}$. The distorted dislocations are 4|6 and 6|8 rings. The relaxed simulation cell sizes are $a = 98.92$ Å and $b = 24.74$ Å.

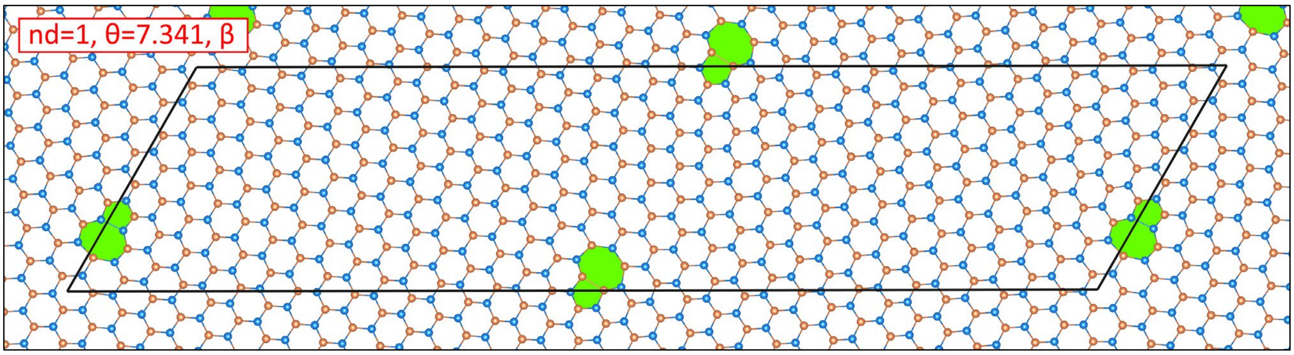


**Figure S3-1-5b.** GB model of family $n_d = 1$ and misorientation angle $\theta = 7.341^{\circ}$. The distorted dislocations are 5|7 rings. The relaxed simulation cell sizes are $a = 98.60$ Å and $b = 24.75$ Å.

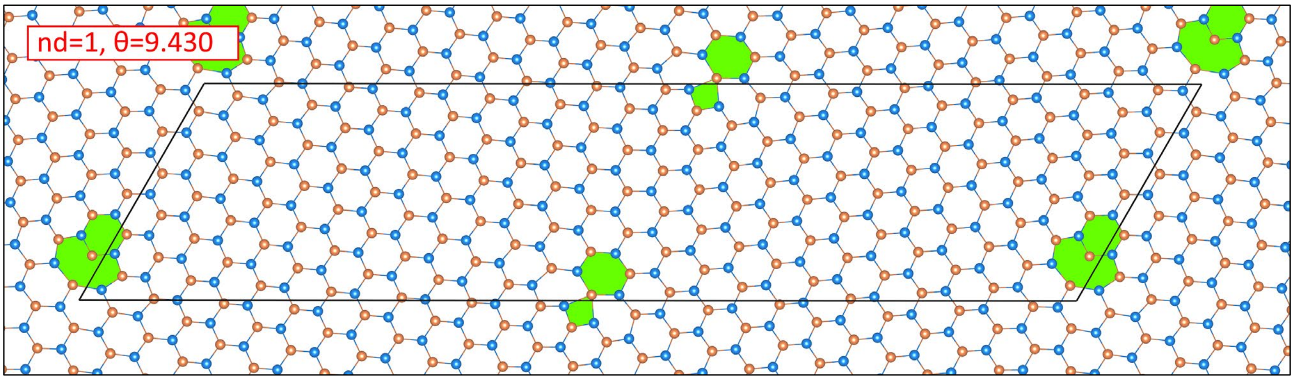


**Figure S3-1-6.** GB model of family $n_d = 1$ and misorientation angle $\theta = 9.430^{\circ}$. The relaxed simulation cell sizes are $a = 76.83$ Å and $b = 19.26$ Å.

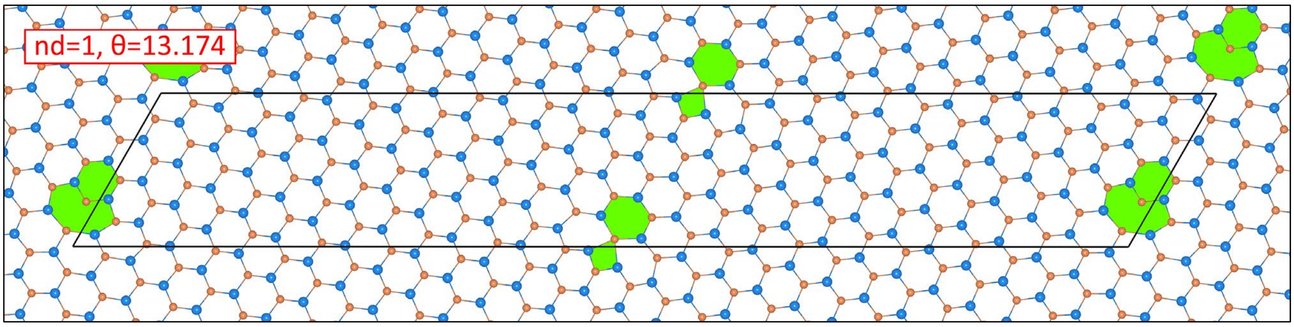


**Figure S3-1-7.** GB model of family $n_d = 1$ and misorientation angle $\theta = 13.174^{\circ}$. The relaxed simulation cell sizes are $a = 82.58$ Å and $b = 13.81$ Å.

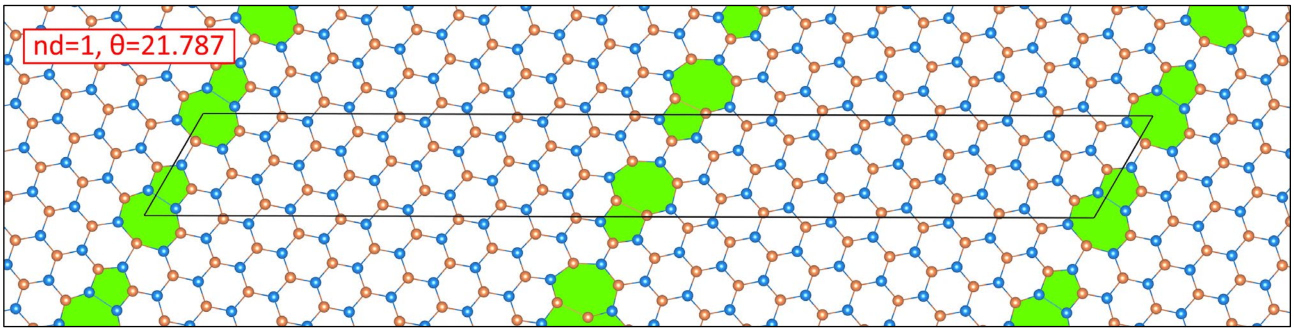


**Figure S3-1-8.** GB model of family $n_d = 1$ and misorientation angle $\theta = 21.787^{\circ}$. The relaxed simulation cell sizes are $a = 67.55$ Å and $b = 8.38$ Å.

### 3.2. The family of $n_d = 2$

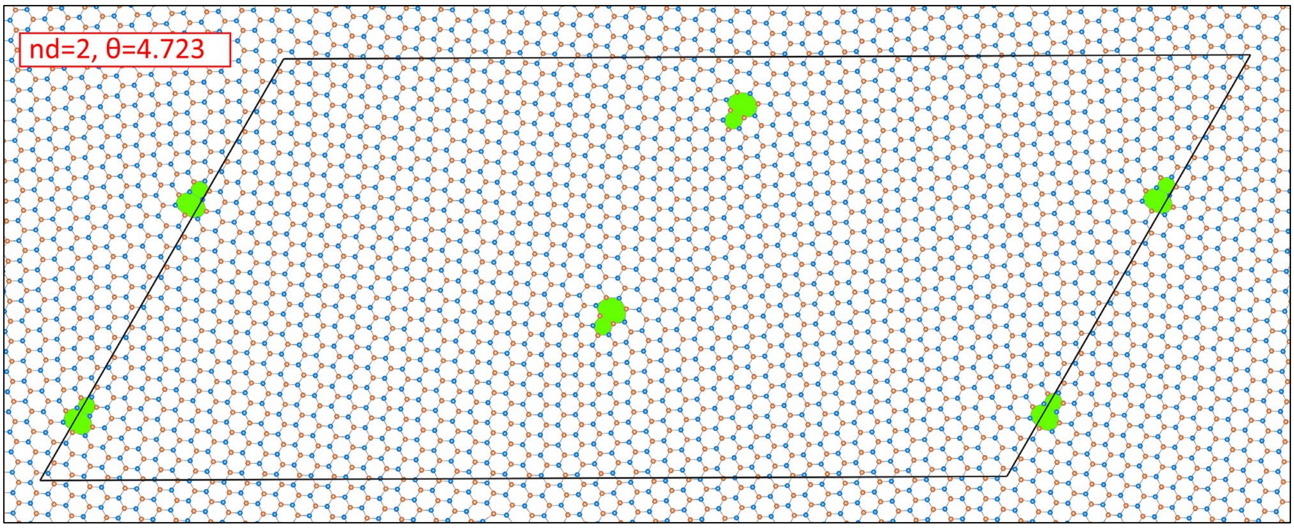


**Figure S3-2-1.** GB model of family $n_d = 2$ and misorientation angle $\theta = 4.723^{\circ}$. The relaxed simulation cell sizes are $a = 152.44$ Å and $b = 76.83$ Å.

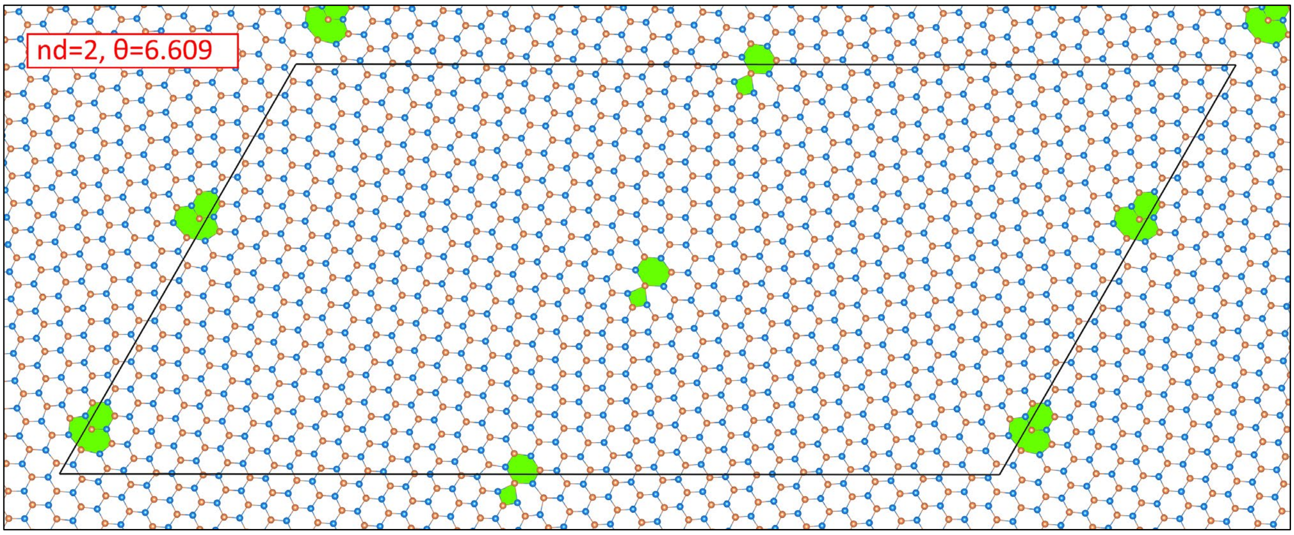


**Figure S3-2-2.** GB model of family $n_d = 2$ and misorientation angle $\theta = 6.609^{\circ}$. The relaxed simulation cell sizes are $a = 109.10$ Å and $b = 54.89$ Å.

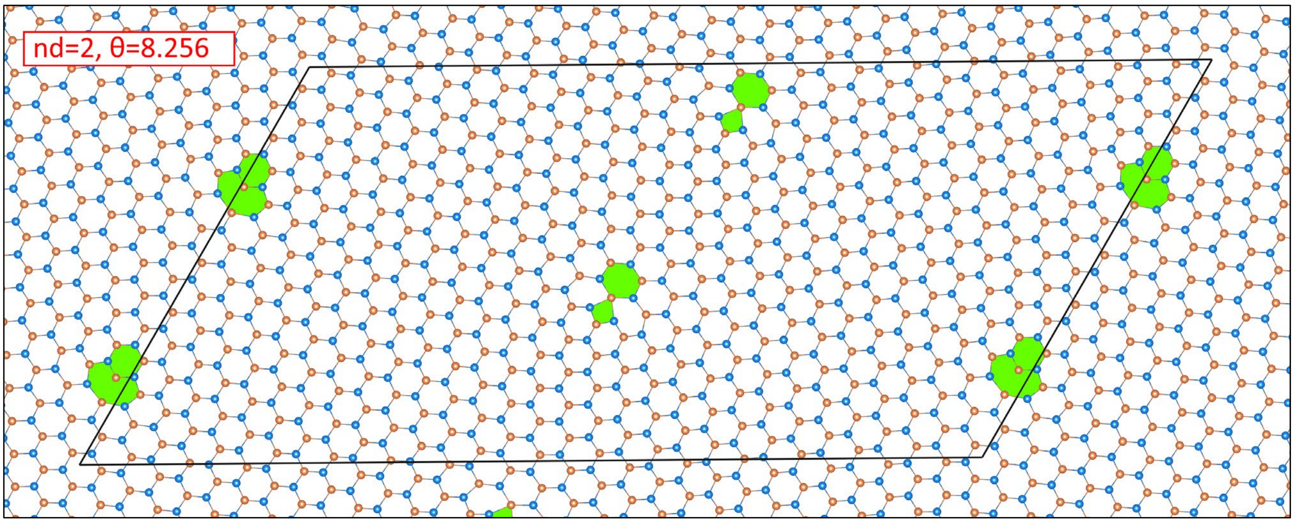


**Figure S3-2-3.** GB model of family $n_d = 2$ and misorientation angle $\theta = 8.256^{\circ}$. The relaxed simulation cell sizes are $a = 86.45$ Å and $b = 44.02$ Å.

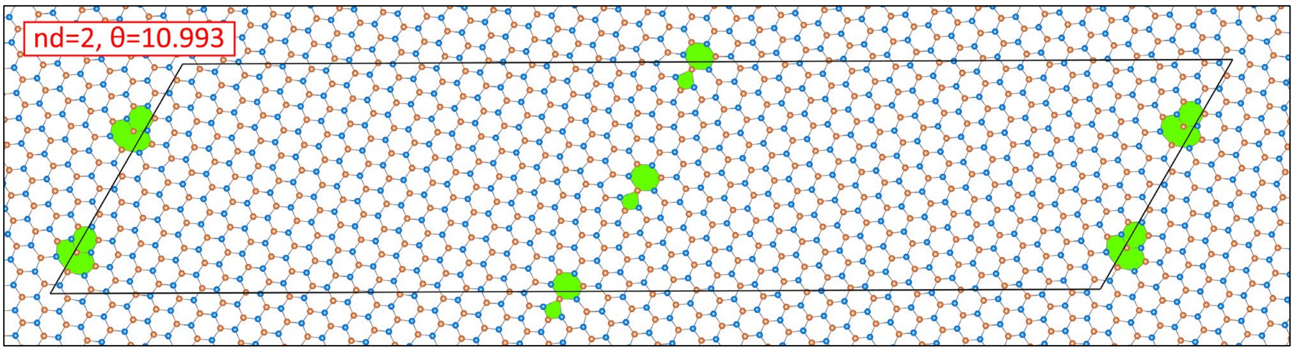


**Figure S3-2-4.** GB model of family $n_d = 2$ and misorientation angle $\theta = 10.993^{\circ}$. The relaxed simulation cell sizes are $a = 131.18$ Å and $b = 33.08$ Å.

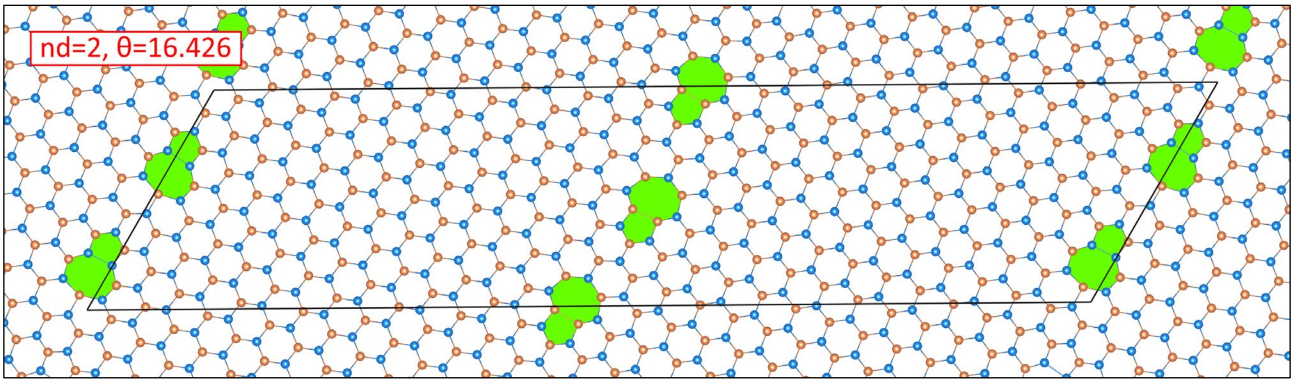


**Figure S3-2-5.** GB model of family $n_d = 2$ and misorientation angle $\theta = 16.426^{\circ}$. The relaxed simulation cell sizes are $a = 87.74$ Å and $b = 22.19$ Å.

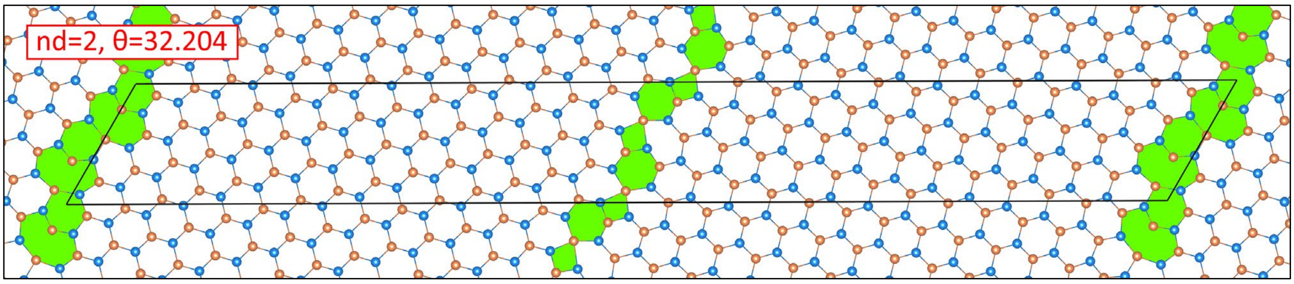


**Figure S3-2-6.** GB model of family $n_d = 2$ and misorientation angle $\theta = 32.204^{\circ}$. The relaxed simulation cell sizes are $a = 90.42$ Å and $b = 11.41$ Å.

### 3.3. The family of $n_d = 3$

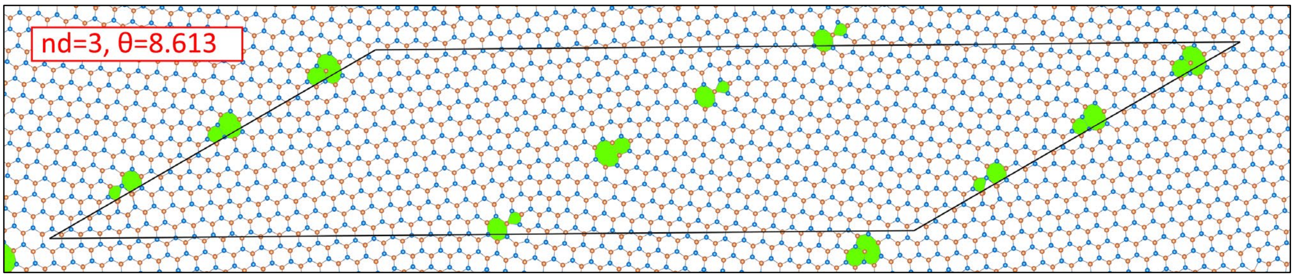


**Figure S3-3-1.** GB model of family $n_d = 3$ and misorientation angle $\theta = 8.613^{\circ}$. The relaxed simulation cell sizes are $a = 145.32$ Å and $b = 63.25$ Å.

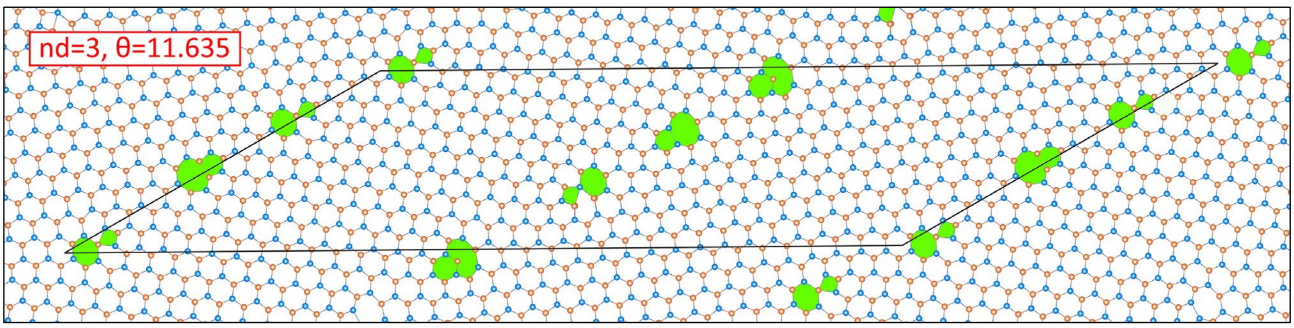


**Figure S3-3-2.** GB model of family $n_d = 3$ and misorientation angle $\theta = 11.635^{\circ}$. The relaxed simulation cell sizes are $a = 107.77$ Å and $b = 46.89$ Å.

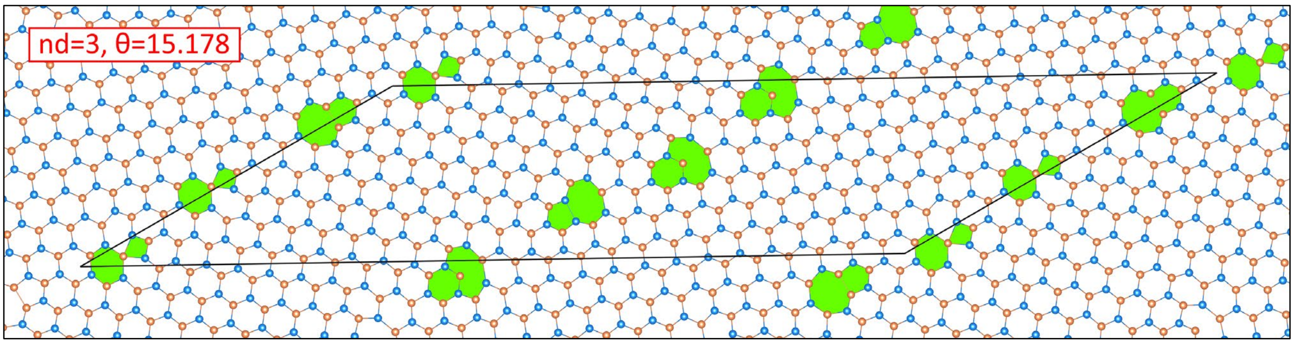


**Figure S3-3-3.** GB model of family $n_d = 3$ and misorientation angle $\theta = 15.178^{\circ}$. The relaxed simulation cell sizes are $a = 82.37$ Å and $b = 36.01$ Å.

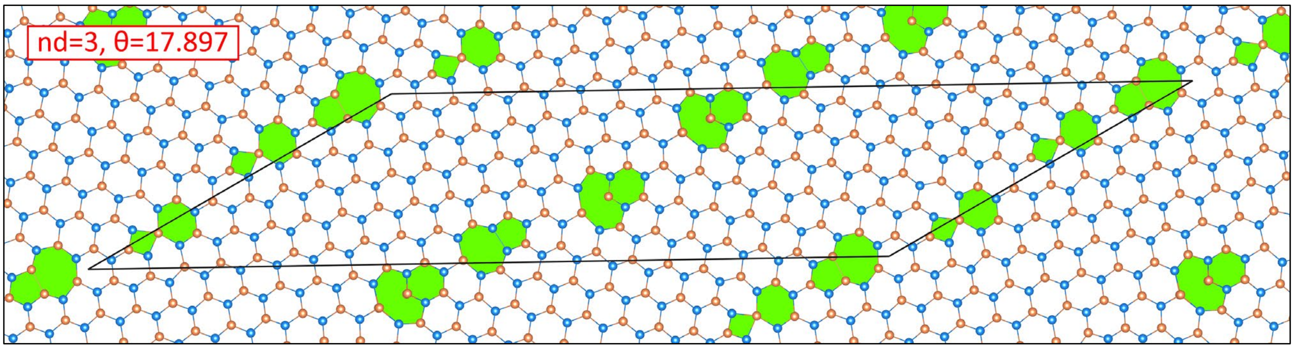


**Figure S3-3-4.** GB model of family $n_d = 3$ and misorientation angle $\theta = 17.897^{\circ}$. The relaxed simulation cell sizes are $a = 69.97$ Å and $b = 30.59$ Å.

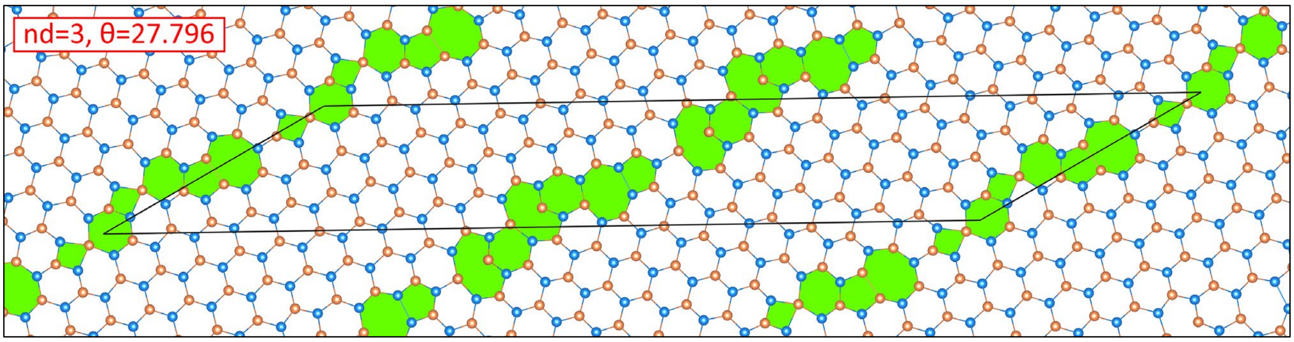


**Figure S3-3-5.** GB model of family $n_d = 3$ and misorientation angle $\theta = 27.796^{\circ}$. The relaxed simulation cell sizes are $a = 67.97$ Å and $b = 19.76$ Å.

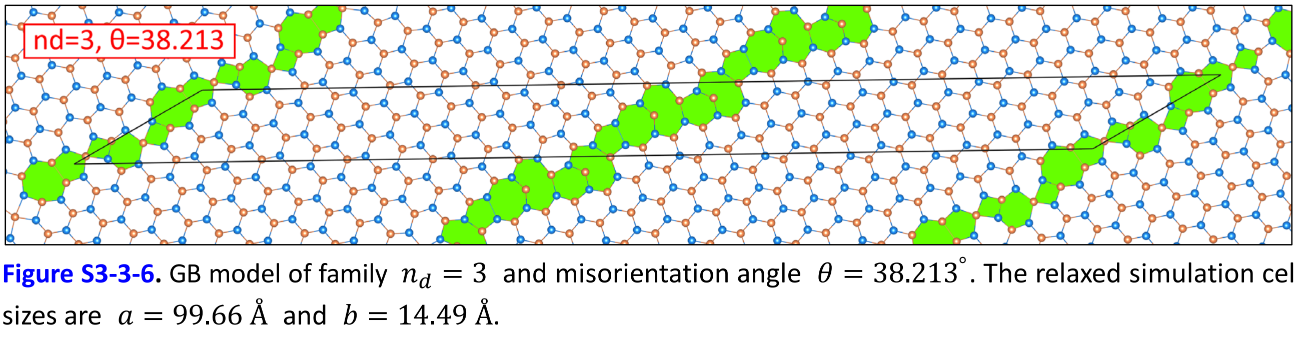


**Figure S3-3-6.** GB model of family $n_d = 3$ and misorientation angle $\theta = 38.213^{\circ}$. The relaxed simulation cell sizes are $a = 99.66$ Å and $b = 14.49$ Å.

### 3.4. The family of $n_d = 4$

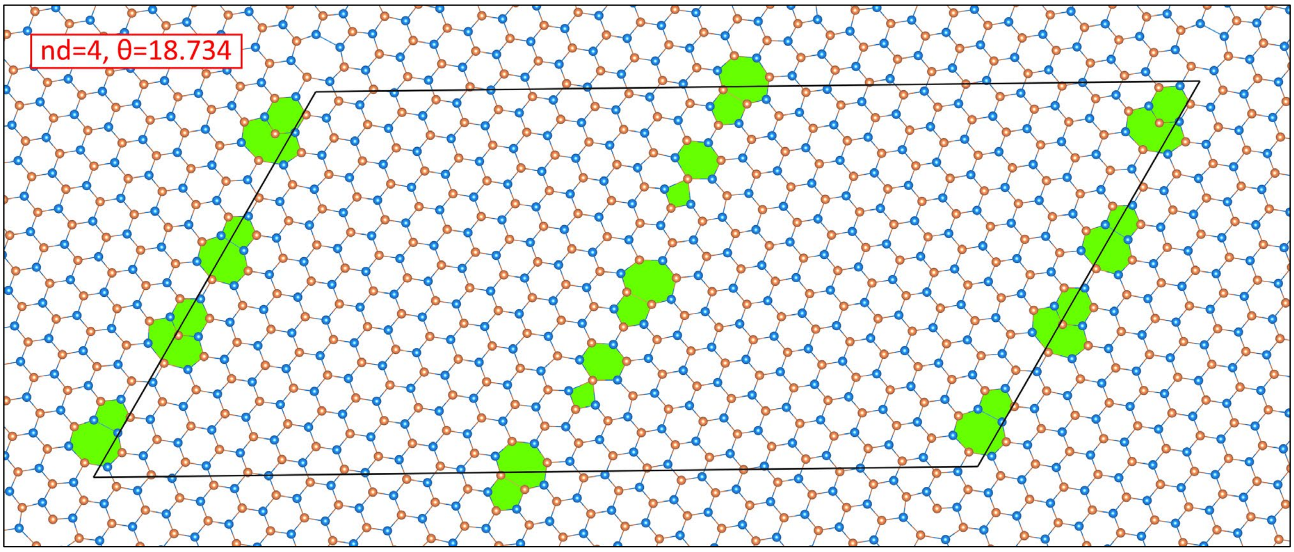


**Figure S3-4-1.** GB model of family $n_d = 4$ and misorientation angle $\theta = 18.734^{\circ}$. The relaxed simulation cell sizes are $a = 76.79$ Å and $b = 38.60$ Å.

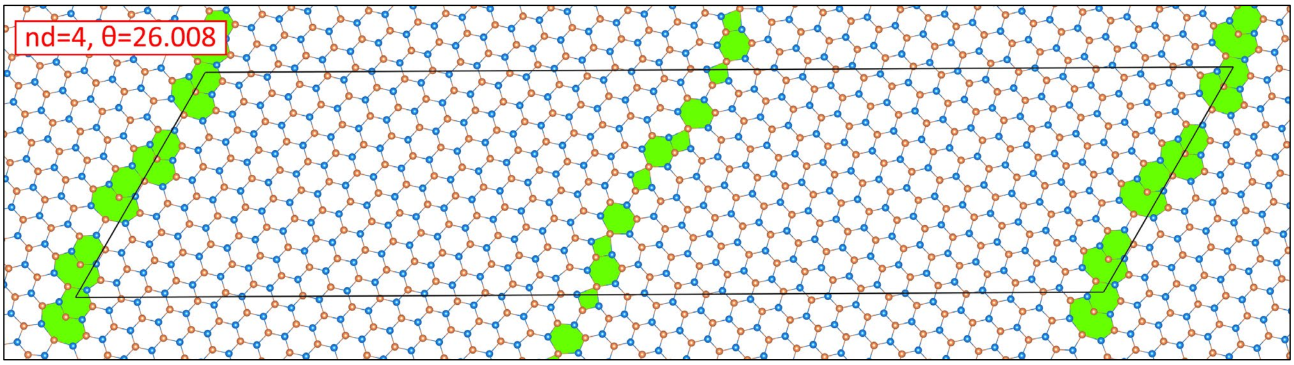


**Figure S3-4-2.** GB model of family $n_d = 4$ and misorientation angle $\theta = 26.008^{\circ}$. The relaxed simulation cell sizes are $a = 111.38$ Å and $b = 28.13$ Å.

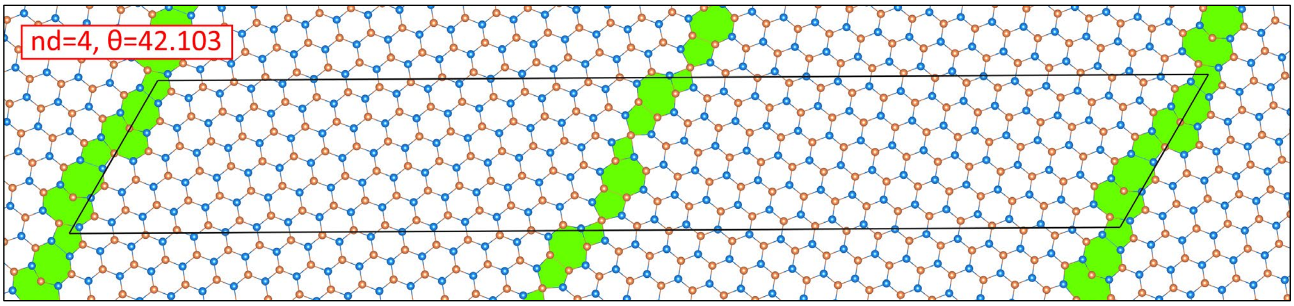


**Figure S3-4-3.** GB model of family $n_d = 4$ and misorientation angle $\theta = 42.103^{\circ}$. The relaxed simulation cell sizes are $a = 104.65$ Å and $b = 17.62$ Å.

## 4. Weak magnetic instability

Magnetic moment could be strongly underestimated by the conventional LDA and GGA functional due to the well-known self-interaction error. This is significantly improved by the recently-developed SCAN (stands for *Strongly Constrained and Appropriately Normed* [5])meta-GGA, as established in our previous work in transition-metal mono-oxides [4]. Here, we use SCAN implemented in FHI-aims [3] to evaluate the magnetic moments of two systems.

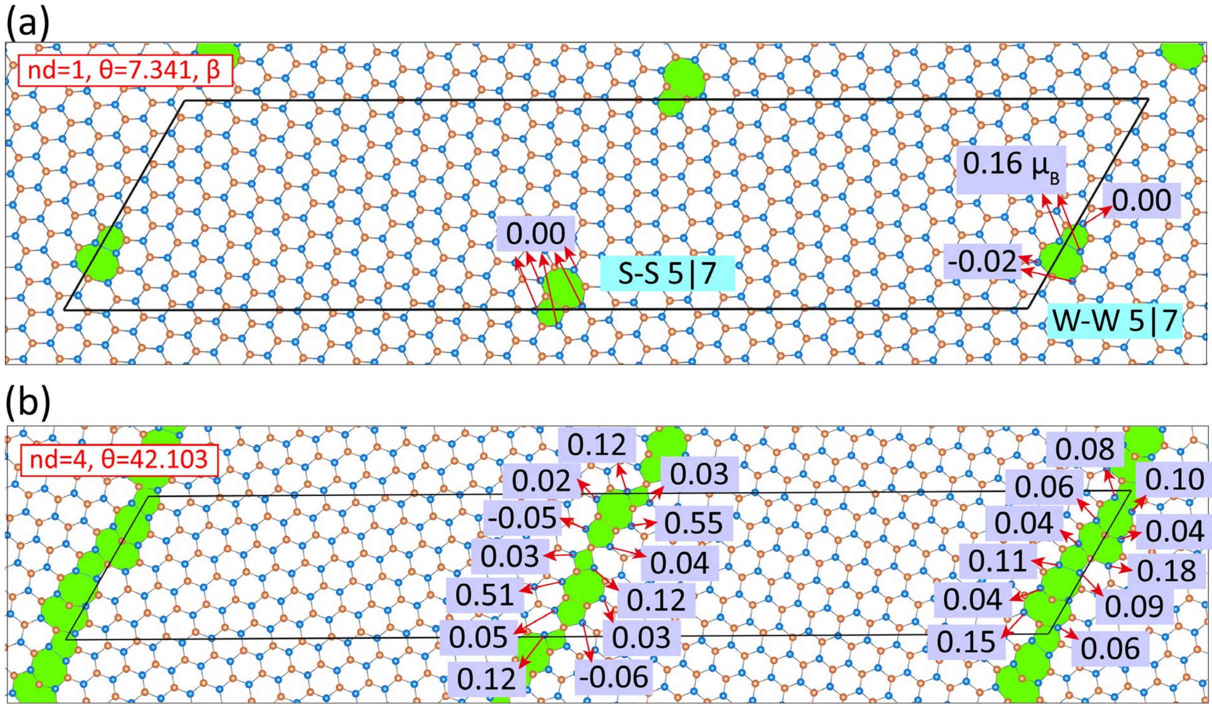


**Figure S4.** Magnetic moments calculated using the SCAN meta-GGA for two GB models. **(a)** Family $n_d = 1$ and the misorientation angle $\theta = 7.341^{\circ}$. **(b)** Family $n_d = 4$ and the misorientation angle $\theta = 42.103^{\circ}$. The magnetic moments of W atoms are shown in the unit of $\mu_B$.

## 5. Deriving the critical angle by fitting to the Read-Shockley relation

Carlsson et al. calculated the formation energies of graphene GBs [6], covering various misorientation angles in the range $0^{\circ} < \theta \leq 60^{\circ}$. They found the Read-Shockley relation for low-angle GBs [7] is valid up to $\theta_c = 12^{\circ}$. However, we argue that the critical angle could be extended to a higher value of $\theta_c \approx 20^{\circ}$, as shown in Figure S5(a). Too strict fitting criteria might have been used in Ref [6]. Following the same approach, we derive a critical angle of $\theta_c \approx 14^{\circ}$ for the $WS_2$-GBs [Figure S5(b)].

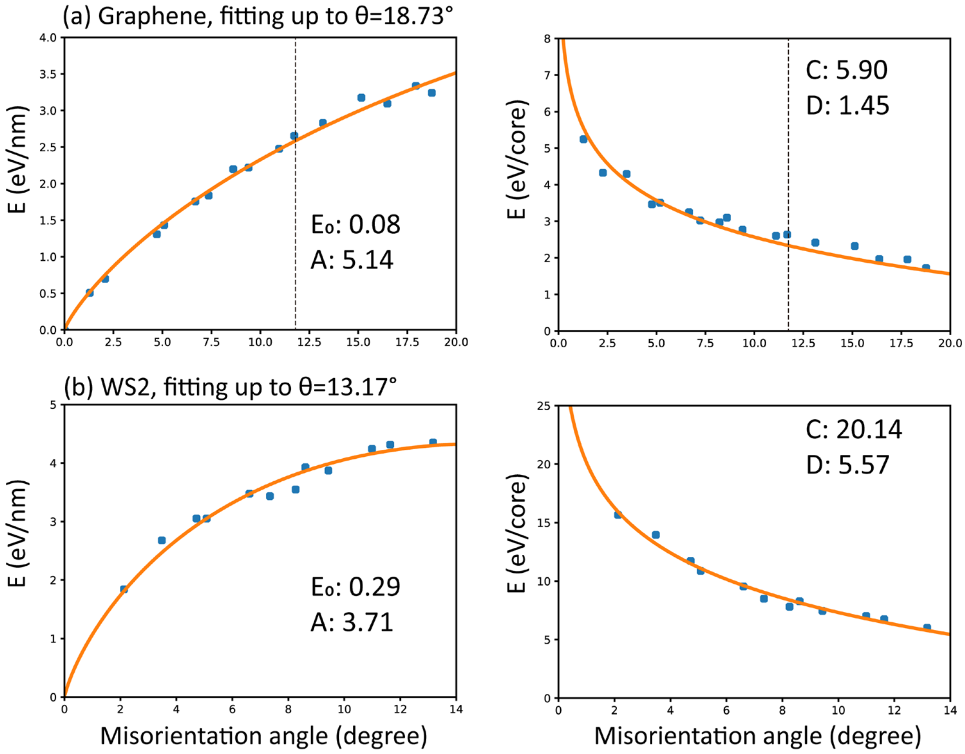


**Figure S5.** Agreement of the calculated data with the Read-Shockley relation. **(a)** Graphene results fitted up to the angle $\theta = 18.73^{\circ}$. **(b)** $WS_2$ results fitted up to $\theta = 13.17^{\circ}$.

## References


1. José M. Soler, Emilio Artacho, Julian D. Gale, Alberto García, Javier Junquera, Pablo Ordejón, and Daniel Sánchez-Portal, *The SIESTA method for ab initio order-N materials simulation.* Journal of Physics: Condensed Matter. **14**, 2745-2779 (2002).
2. John P. Perdew, Kieron Burke, and Matthias Ernzerhof, *Generalized Gradient Approximation Made Simple.* Physical Review Letters. **77**, 3865-3868 (1996).
3. Volker Blum, Ralf Gehrke, Felix Hanke, Paula Havu, Ville Havu, Xinguo Ren, Karsten Reuter, and Matthias Scheffler, *Ab initio molecular simulations with numeric atom-centered orbitals.* Computer Physics Communications. **180**, 2175-2196 (2009).
4. Yubo Zhang, James Furness, Ruiqi Zhang, Zhi Wang, Alex Zunger, and Jianwei Sun, *Symmetry-breaking polymorphous descriptions for correlated materials without interelectronic U.* Physical Review B. **102**, 045112 (2020).
5. Jianwei Sun, Adrienn Ruzsinszky, and John P Perdew, *Strongly Constrained and Appropriately Normed Semilocal Density Functional.* Physical Review Letters. **115**, 036402 (2015).
6. Johan M. Carlsson, Luca M. Ghiringhelli, and Annalisa Fasolino, *Theory and hierarchical calculations of the structure and energetics of [0001] tilt grain boundaries in graphene.* Physical Review B. **84**, (2011).
7. W. T. Read and W. Shockley, *Dislocation Models of Crystal Grain Boundaries.* Physical Review. **78**, 275-289 (1950).